Geomorphology 379 (2021) 107626

Contents lists available at ScienceDirect

Geomorphology

journal homepage: www.elsevier.com/locate/geomorph

Morphological characteristics and changes of two meandering rivers in the Qinghai-Tibet Plateau, China

Xiwei Guo [a], Peng Gao [a,*], Zhiwei Li [b]

[a] Department of Geography and the Environment, Syracuse University, Syracuse, NY 13244, USA
[b] State Key Laboratory of Water Resources and Hydropower Engineering Science, Wuhan University, Wuhan, Hubei 430072, China

ARTICLE INFO

Article history:
Received 29 November 2020
Received in revised form 22 January 2021
Accepted 25 January 2021
Available online 28 January 2021

Keywords:
Meandering river
Planform geometry
Lateral migration
Qinghai-Tibet Plateau

ABSTRACT

This study investigated bend morphology and dynamic changes of two highly convoluted meandering rivers, the Black River and the White River, in the Upper Yellow River Watershed of the Qinghai-Tibet Plateau (QTP), China. Using remotely sensed data, we characterized channel morphology and lateral changes of 290 meander bends in the two rivers. These bends exhibited extensive development of compound structures with each involving multiple sub-bends. Their migration patterns were dominated by extension, translation, and the combination of both, with the average migration rate higher in bends that changed by translation than that of bends by other modes. These morphological changes led to a longitudinal erosion-to-deposition pattern along the two studied rivers. Our analyses showed that the White River migrated much faster with more frequent cutoffs but fewer compound bends than the Black River, which may be attributed to the greater stream power of the former. We found a similar single-mode relationship between migration rate and bend curvature, commonly reported in previous studies, indicating that the largest migration rate occurred in bends with medium curvatures. This relationship, however, was altered to a quasi-monotonic inverse one when the average migration rates of bends were calculated for each class interval of bend curvatures, suggesting the complexity of bend morphodynamics. In general, the two studied meandering rivers migrated slower than many other meandering rivers worldwide, which allowed their bends to evolve into complex planform structures.

1. Introduction

Meandering rivers encompass a broad spectrum of single-threaded channels that exhibit various sinuous planform patterns (Leopold and Wolman, 1960; Schumm, 1985; Hooke, 2013). They are typically developed in alluvial environments and repeatedly migrate over floodplains (Hooke, 1984; Howard, 1992; Nicoll and Hickin, 2010). A river channel may be defined as "meandering" when its sinuosity is >1.3-1.5, although a single, clear threshold value of sinuosity is hard to be determined because it is scale-dependent (Chang, 1984; Ebisemiju, 1994). Meandering channels may increase their sinuosity by lateral migration and decrease it by cutoff (Ikeda et al., 1981; Hickin and Nanson, 1984; Constantine and Dunne, 2008; Güneralp and Rhoads, 2009). Spatial and temporal patterns of meanders are controlled by hydrogeomorphic properties of channels and floodplains, which arise from complex interactions among river flow, sediment transport, channel morphology, and floodplain characteristics (Ferguson, 1975; Dietrich et al., 1979; Anthony and Harvey, 1991; Simon and Collison, 2002; Perucca et al., 2007; Hooke, 2013; Constantine et al., 2014; Schwendel et al., 2015).

Research on forms and processes of meandering channels includes empirical and theoretical analyses for explaining and predicting patterns of meander morphology and its changes at multiple spatial and temporal scales (Stølum, 1996; Güneralp et al., 2012; Hooke, 2013; Church and Ferguson, 2015). While empirical studies aim to characterize meander processes from different aspects, such as bank erosion, bar formation, cutoff, and, more generally, lateral migration (e.g., Nanson, 1980; Thorne, 1991; Frothingham and Rhoads, 2003; Constantine et al., 2014; Li and Gao, 2019a), theoretical approaches rely on experimental or numerical models to simulate morphodynamic processes involved in meander evolution (e.g., Ikeda et al., 1981; Zolezzi and Seminara, 2001; Darby et al., 2002). Many of these studies highlighted hydrologic processes in controlling channel morphological adjustment (e.g., Dietrich, 1987; Markham and Thorne, 1992), whereas others focused on revealing kinematic linkages between bend morphology and migration (e.g., Parker et al., 1983; Hickin and Nanson, 1984; Hudson and Kesel, 2000; Hooke, 2007). Experimental and modeling outcomes are typically supported by in-situ measured data and/or planform morphology of specific meandering rivers (e.g., Howard and Knutson, 1984; Lancaster and Bras, 2002), which lead to an enduring limitation: the findings lack generalization (Güneralp and Marston, 2012). The main reason for this limitation is that repetitively measuring meander

* Corresponding author.
E-mail address: pegao@maxwell.syr.edu (P. Gao).

https://doi.org/10.1016/j.geomorph.2021.107626
0169-555X/

channel morphology and its temporal changes is labor intensive and thus could not be widely deployed in practice. For instance, it is well known that bend migration is not only controlled by intensified shear stress along the outer bank but also affected by bar development as the latter changes flow structure (Seminara, 2006). Yet, measuring these hydraulic parameters and bend morphology over time is pragmatically difficult because of the obvious logistic challenges, though there have been very limited studies on detailed velocity distribution in channel cross sections and spatial variations of bank properties along a meander bend (Frothingham and Rhoads, 2003; Zinger et al., 2013; Konsoer et al., 2016). Therefore, using satellite imagery to effectively extract bend morphology over various spatial and temporal ranges, and to understand how meander planform patterns are tied to its lateral migration is still popular in current research frontiers (Hooke and Yorke, 2010; Ollero, 2010; Gilvear and Bryant, 2016; Schwenk et al., 2017; Guo et al., 2019; Ielpi and Lapôtre, 2019).

Studies in the past five decades have advanced our knowledge in: (1) quantifying bend geometry using morphological metrics such as bend amplitude, wavelength, and curvature (e.g., Magdaleno and Fernández-Yuste, 2011; Yousefi et al., 2016); (2) determining diverse trajectories of bend migration using a typology of bend change (e.g., Hooke and Harvey, 1983; Morais et al., 2016); (3) understanding the lag between locations of maximum bend curvature and migration rate, and their relationships (e.g., Nanson and Hickin, 1983; Güneralp and Rhoads, 2009; Sylvester et al., 2019). Nonetheless, we are far from reaching general models that enable the prediction of the evolution of meandering rivers under various environments. We are still missing two pieces in our current understanding of meandering rivers with regards to river environments and the complexity of river planform. First, though meandering rivers with complex planform structures have been noted and studied (e.g., Frothingham and Rhoads, 2003; Gautier et al., 2007; Hooke, 2013), their patterns of channel morphology and dynamics are not yet fully understood. Second, meandering rivers in temperate and tropical lowland environments have been extensively investigated, but little attention has been paid to those developed in high-elevation environments where the hydrological regime, land cover, and other hydrogeomorphic factors may be different.

We investigated morphological characteristics and dynamic changes of two meandering rivers with complex planform structures in the Upper Yellow River Watershed, located in eastern QTP of western China (Fig. 1a). In particular, we attempted to achieve three objectives: (1) to characterize channel planform morphology of the two meandering rivers; (2) to reveal patterns of channel morphological and morphodynamic changes; (3) to assess geomorphological differences between the two rivers and among other meandering rivers in the world.

2. Materials and methods

2.1. Study area

Sourced from the Bayan Har Mountains in northeastern QTP, the Upper Yellow River runs for about 600 km until arriving at the "First Great Bend" where the two main tributaries, the Black and the White rivers, converge (Fig. 1b). The contributing areas of the two rivers form the Zoige Basin whose mean elevation is approximately 3400 m. The Zoige Basin has a relatively flat topography surrounded by high mountains formed around 14 million years ago owing to orographic activities (Nicoll et al., 2013). The basin is filled with lacustrine deposits that are at least 30 m deep (Chen et al., 1999), allowing local rivers to develop alluvial channels. The Zoige basin has a typical highland climate and is strongly influenced by the East Asian Monsoon that brings precipitation during the summer months. The Black and the White rivers both originate from the Minshan Mountains and generally flow northward through the Zoige Basin with the former situated in the north and the latter in the south (Fig. 1b). Their drainage areas are 7600 and 5500 km^2, respectively, and their mean annual discharges at the outlets are 58 and 56 m^3/s, respectively.

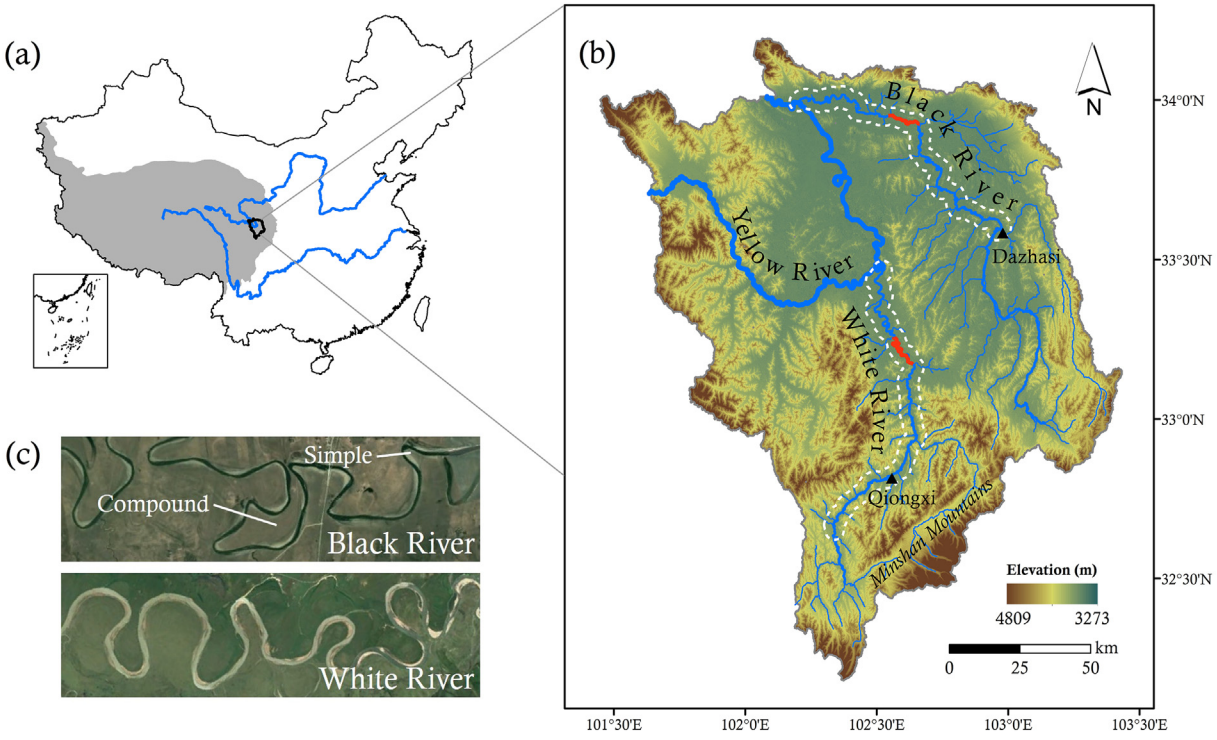

Fig. 1. Overview of the study area. (a) Qinghai-Tibet Plateau (the shaded area) and the Zoige Basin (the outlined area) in China; (b) Geomorphology of the Zoige Basin and locations of the studied reaches (within dotted lines); (c) Plan view of a section of each studied river (their locations are marked in red in (b)) and examples of simple and compound bends in the Black River.

This study focused on the middle and lower reaches of the two rivers (i.e., the lower Black River and the lower White River) where meandering channels are extensively developed. Their floodplains feature ample oxbow lakes and are covered by uniformly distributed peat or grass. Specifically, the studied reach of the Black River starts at the first upstream confluence where the Requ River joins the Black River in the Town of Dazhasi and ends at the outlet of the Black River (Fig. 1b). The total channel length is approximately 240 km. For the White River, we studied the lowermost 190 km reach before it enters the Upper Yellow River (Fig. 1b). The reach-averaged sinuosity of the lower Black and White rivers are 2.03 and 1.63, respectively, though their local channel segments commonly have higher sinuosity (>2.0). Their average channel widths are 86 and 91 m, respectively. The lower Black River develops many compound bends with convoluted loops that form highly sinuous channels, whereas the lower White River has fewer compound bends but more mid-channel and lateral bars, especially near the downstream end (Fig. 1c). The average channel gradients are 0.09‰ and 0.4‰ for the studied reaches of the Black and the White rivers, respectively. Lateral migration and cutoff are the predominant processes shaping their planform structures with the latter dominated by neck cutoff. Both studied reaches are gravel-bedded and have comparable grain size distributions in channel banks and beds. Banks along the two studied reaches have a two-layer vertical structure with the top one comprised of soil-vegetation (peat or grass) mixture and the lower one comprised of fine sand and silt (the average median particle size is 89 μm based on analysis of particle size distribution from several field-collected samples) that are graded into the bank toe formed by fine gravels. Because the top mixed layer has a much higher resistance to fluvial erosion than the lower layer does, channel banks often form cantilever arms. Therefore, cantilever failure caused by continuous fluvial erosion is the key mechanism of bend evolution in the Zoige Basin (Li and Gao, 2019a).

The two studied reaches largely remain undisturbed. Human activities in the Zoige Basin are primarily grazing. Along the main channels of the two rivers, the only two towns, Qiongxi (Hongyuan County seat) and Dazhasi (Zoige County seat), have a population of around 10,000 in each. The greatest environmental change within the Zoige Basin over the past few decades was wetland degradation, which was mainly attributed to the excavation of artificial ditches between the 1960s and 1990s that had drained 57.7% of peatland areas as of 2015 and gully erosion on hillslopes (Qiu et al., 2009; Li et al., 2018; Li and Gao, 2019b; Li et al., 2019). In general, channels of the two rivers largely remain in pristine conditions.

2.2. Methods

2.2.1. Data acquisition and error assessment

Using Landsat Thematic Mapper (TM) and Operational Land Imager (OLI) data with a spatial resolution of 30 m, we extracted channel planform morphology in 1986 and 2017. The data selected were acquired in the summer when cloud cover was minimal and the water level was high, such that meander bends along the reaches may be clearly identified. Because the rate of channel migration in the studied reaches was relatively small, an observation from our preliminary study, the selected satellite imagery of 1986 and 2017, spanning over 31 yr, was sufficient to capture changes in the meander bends. Because several segments of the channels in both studied reaches (accounting for <5% of total channel lengths) were not identifiable because of cloud cover in the 1986 data, an additional TM image obtained in summer 1990 was used for compensation. The satellite images were then imported into ArcGIS where channel banks and centerlines were digitized. The bank lines were digitized according to the identified vegetation boundaries along the channels that best represent channel bankfull width (e.g., Winterbottom, 2000; Frias et al., 2015; Donovan et al., 2019). These vegetation boundaries were determined using the Normalized Distribution Vegetation Index (NDVI) based on a threshold of 0.2 (Bertoldi et al., 2011; Henshaw et al., 2013) such that areas with pixel values smaller than the NDVI threshold were identified as river channels. This included both water surfaces and bars. Channel centerlines were then delineated based on identified bank lines.

Two main types of uncertainties are associated with data acquisition and processing in this study. The first was the registration error from the original satellite images, which could be viewed in the metadata. The Root Mean Square Error (RMSE) for data registration was 6.95 and 7.83 m for the 1986 and 2017 images, respectively. These errors accounted for <10% of the average channel width for both studied reaches. The second type of uncertainty may arise during the process of channel digitization, which we assessed by calculating the mean lateral displacement of a section of channel bank from 50 times of re-digitization under the same scale (Downward et al., 1994). We found that the digitizing error was 2.3 m (±0.65) under the scale of 1:10,000. The total error (E_t) could be subsequently calculated by:

$$E_t = \sqrt{{E_1}^2 + {E_2}^2} \quad (1)$$

where E_1 and E_2 denote registration and digitizing errors, respectively. In this study, the calculated E_t was 7.32 and 8.16 m for the images of 1986 and 2017, respectively. Therefore, any linear distance of channel morphology and lateral change <10 m was neglected and treated as zero.

2.2.2. Bend identification and morphometric analysis

Meander bends were identified based on channel centerlines at the initial condition of the study period (i.e., 1986). A bend was identified where there is an arc of at least 60° along the channel centerline (Brice, 1974). All qualified arcs were subsequently classified as either simple bends or sub-bends of compound bends. Although a simple bend only contains one qualified arc, a compound bend contains multiple qualified arcs adjacent to each other. A potential problem associated with the classification of meander bend morphology is that quantitatively distinguishing compound bends from simple bends is difficult. For instance, a given channel segment with multiple qualified arcs may be identified as a single compound bend that involves multiple sub-bends or as multiple simple bends developed in a row. Therefore, we determined that a compound bend may be identified by two conditions: (1) where a bend neck (the narrowest part of the bend) is present and the neck width (w_n) is smaller than ten times the average channel width (w) at the neck (Fig. 2a); (2) if a bend neck is not present, the radii of qualified arcs (O_1, O_2, etc.) are located on the same side (i.e., the left or right bank) of the channel and the distance between any two adjacent radii is less than ten times of average w at bend apices (Fig. 2b). In the first condition, all qualified arcs beyond the bend neck are identified as sub-bends of the compound bend, as marked by dotted circles. This distance threshold (i.e., 10w) was determined based on our preliminary study of the meander bends. Although it may be subjective, it was sufficient for effective bend classification in the lower Black and White rivers.

The planform morphology of each bend was then characterized using bend amplitude (A_w) and wavelength (L_w) (Magdaleno and Fernández-Yuste, 2011) (Fig. 2c), which captures the degree of bend elongation and widening, respectively. Both parameters were normalized with w of each bend apex. For compound bends, A_w was measured from the farthest sub-bend and was normalized by the average w at bend apices of all sub-bends in the compound bend. Both A_w and L_w were used to compare statistically between the two types of bends (i.e., simple and compound) and between the two rivers. The parameters were also plotted against longitudinal distance, which was measured in downstream direction as valley length, rather than the channel length. Radius of curvature of meander bends (r_m) was measured for all identified bends by drawing circles that fit the arcs previously used for bend identification (e.g., Brice, 1974; Hooke, 1984;

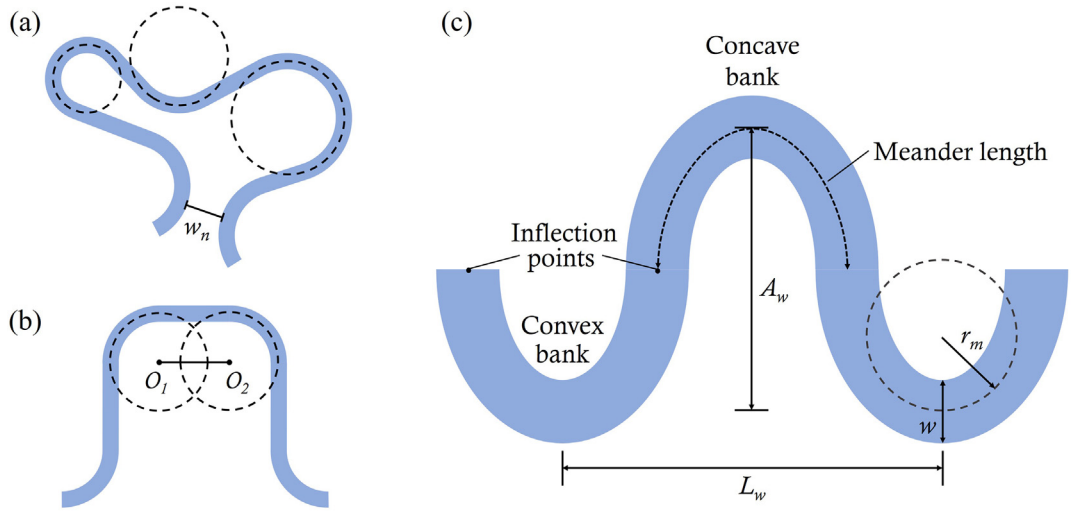

Fig. 2. Bend morphology and morphometric parameters. (a) Identification of a compound bend when a bend neck is present; (b) Identification of a compound bend without a bend neck. Shapes of the compound bends are based on Fig. 1H and P in Brice (1974); (c) Definition of morphometric parameters in ideal sine-curved meander bends.

Nicoll and Hickin, 2010) (Fig. 2c). For compound bends, r_m was measured for each individual sub-bend. Meander bend curvature (r_m/w) was then calculated by normalizing r_m with w at bend apices.

2.2.3. Analysis of channel morphological changes

Morphological changes of the studied reaches were characterized based on the typology (Hooke and Harvey, 1983; Hooke, 1984) describing relative positions of the same bend in the beginning (i.e., 1986) and ending (i.e., 2017) year (Fig. 3). By superimposing the two extracted centerlines and viewing the positional changes of each bend (sub-bends), we classified patterns of bend changes into four main categories: extension, translation, cutoff, and retraction (Fig. 3). In addition, a significant number of bends in both reaches exhibited a pattern that combined both extension and translation. To reflect their differences with pure extension and pure translation, we created two more categories: extension with translation (ET) and translation with extension (TE). In particular, ET reflected the change of a bend that had migrated for a greater distance in the transverse direction (i.e., towards the floodplain) than in the longitudinal direction (i.e., downstream along the channel), whereas TE represented the change of a bend that had migrated for a greater distance longitudinally than transversely. Other than these types of bend changes, meander bends that involved lateral changes of large, semi-vegetated bars or islands were marked as "conditional" cases in the classification. These large bars and islands were rare in both studied reaches because of the dominant single-thread characteristic of meandering channels.

Meander morphological changes have also been commonly described by calculating the lateral migration rates of meander bends (Hickin and Nanson, 1984; Casado et al., 2016; Alber and Piégay, 2017). We measured lateral migration of all bends between 1986 and

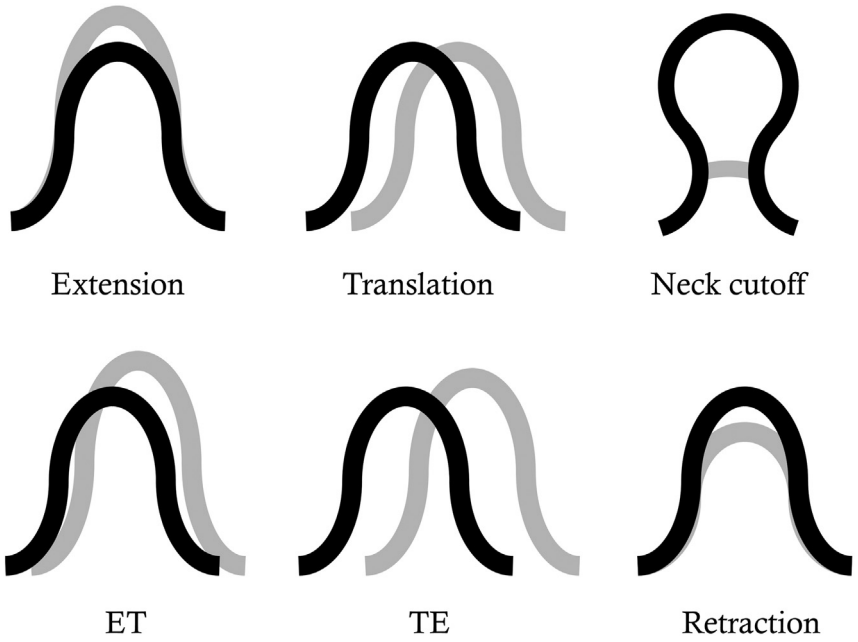

Fig. 3. Major types of meander-bend change observed in the studied reaches of the Black and the White rivers. The black and the grey lines indicate the initial and final positions of the same channel, respectively.

Table 1
Summary of bend identification in the studied reaches.

		Black River	White River
		Number of bends	Number of bends
Total bends		149	141
Simple bends		99	128
Compound bends		50	13
Compound bends with	Two sub-bends	36	10
	Three sub-bends	9	3
	Four sub-bends	5	0

2017 as the maximum displacement along the superimposed channel centerlines of each bend, including each sub-bend. A migration distance <10 m was considered as zero because of potential errors described before. For bends that changed by translation, the lateral migration was measured by linking points with a similar local curvature in each bend because it best reflected dynamic patterns of meander-bend change. In the studied reaches, the maximum migration typically occurred at or immediately downstream of bend apices. The 31-yr total migration was then normalized with w and was statistically summarized among different types of bend change and between the two studied reaches. Because this study only involved one time period (i.e., 1986-2017) for both studied reaches, we used total migration distance over the 31-yr study period for assessment. Migration distances of meander bends that changed by extension, translation, ET, and TE were then plotted against bend curvature to examine their relationships.

2.2.4. Analysis of morphodynamic patterns

In this study, morphodynamic patterns referred to spatial distributions of erosion and deposition in meander bends along the two studied reaches. In particular, an area outside the bank boundary of 1986 but within the boundary of 2017 was considered an erosional area (A_e), whereas that within the bank boundary of 1986 but outside of the boundary of 2017 was considered a depositional area (A_d). Any individual area of erosion or deposition <100 m^2 or with an average width <10 m was neglected owing to the potential uncertainties described before. A_e and A_d were not measured for bends that changed by cutoff and irregular change. We calculated total A_e and A_d, their mean values, and coefficient of variation (CV). We also used the ratio of erosion to deposition (A_e/A_d) of each bend to examine reach-scale morphodynamic patterns with $A_e/A_d > 1$ indicating an erosion-dominated pattern and $A_e/A_d < 1$ indicating a deposition-dominated pattern. For meander bends without deposition (i.e., $A_d = 0$), we manually set $A_d = 1$ to assure that the ratio was mathematically meaningful.

3. Results

3.1. Bend morphology

We identified 149 meander bends in the lower Black River and 141 bends in the lower White River. In the former, 99 were simple bends and the remaining 50 were compound. In the latter, however, 128 bends were simple and only 13 were compound (Table 1). Among the compound bends in both studied reaches, the majority had two sub-bends, making up 72% and 77% of the total in the lower Black and White rivers, respectively. The number of compound bends with three sub-bends accounted for 18% and 23% in the lower Black and White rivers, respectively. Only the lower Black River had five compound bends with each having four sub-bends, accounting for 10% of the total compound bends in the studied reach. In addition to the presence of more sub-bends, the lower Black River also exhibited a cluster pattern for compound bends. Among the 50 compound bends, 40 were distributed next to one another, forming several compound bend clusters with each containing two to six compound bends. By contrast, compound bends in the lower White River were sporadically located over the entire reach and did not exhibit any cluster pattern.

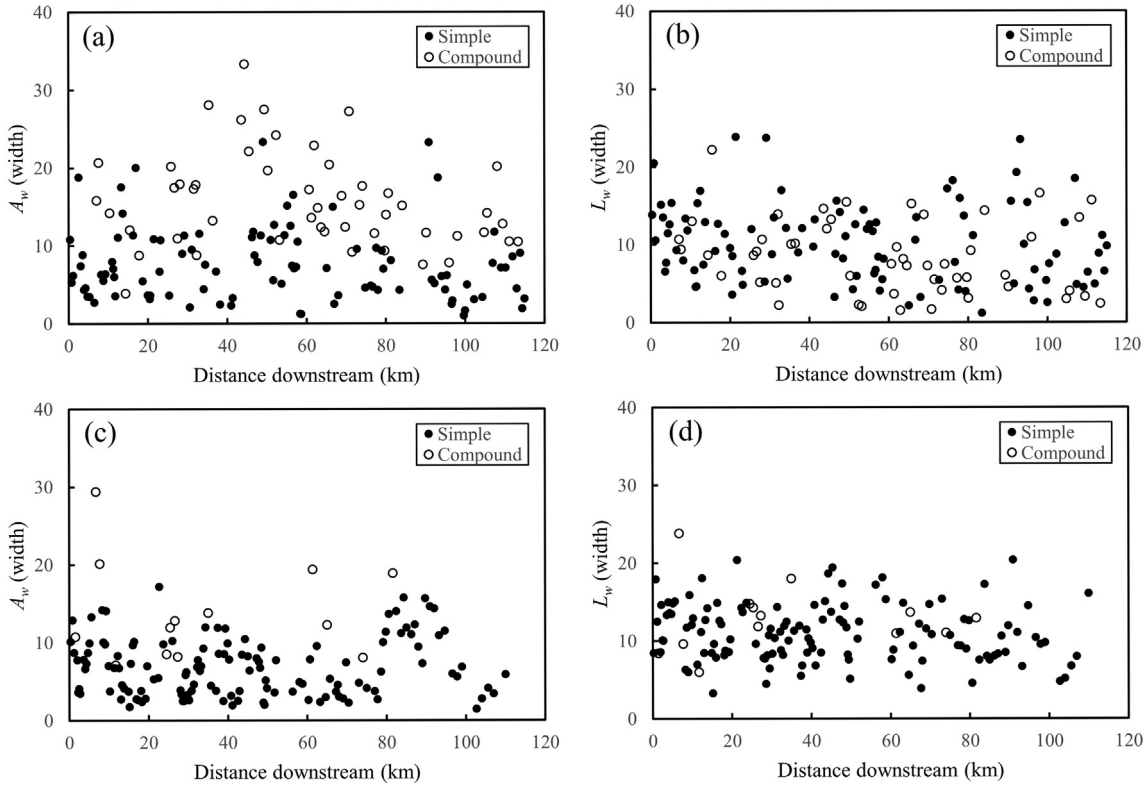

Fig. 4. Longitudinal distributions of width-normalized A_w and L_w of simple and compound bends in the studied reaches of the Black River (a and b) and the White River (c and d).

Table 2
Summary on types of meander bend change in the studied reaches. Each sub-bend of compound bends was analyzed independently for bend change.

Types of bend change	Black River	White River
	Number of bends	Number of bends
Total bends incl. sub-bends	218	157
Extension	100	77
Translation	39	14
Extension with translation	18	5
Translation with extension	15	10
Cutoff	1	9
Retraction	5	3
Conditional extension	2	2
Conditional retraction	3	N/A
Translation with retraction	1	N/A
Irregular change	N/A	15
No change	34	22

In the lower Black River, A_w of simple bends ranged between 1 and 23.3 widths with the mean of 7.6 and *CV* of 0.62. A_w of compound bends ranged between 3.9 and 33.3 widths with the mean of 15.7 and *CV* of 0.39 (Fig. 4a), showing that A_w of simple bends was significantly smaller than that of compound bends ($p < 0.01$), but with greater variability than that of compound bends. In the lower White River, A_w ranged between 1.4 and 17.2 widths for simple bends and between 7.1 and 29.3 widths for compound bends. The mean A_w and *CV* were 6.8 widths and 0.54, respectively, for simple bends, and 13.9 widths and 0.44, respectively, for compound bends (Fig. 4c). Although A_w of simple and compound bends in the lower White River was also significantly different ($p < 0.05$), the difference was relatively less, compared to that between simple and compound bends in the lower Black River.

By contrast, L_w did not differ significantly ($p > 0.05$) between simple and compound bends in both studied reaches. In the lower Black River, L_w ranged between 1.2 and 23.8 widths for simple bends and between 1.5 and 22.2 widths for compound bends. The mean L_w and *CV* were 10.1 widths and 0.49, respectively, for simple bends and 8.4 widths and 0.56, respectively, for compound bends (Fig. 4b). In the lower White River, L_w ranged between 3.3 and 20.4 widths for simple bends and between 6 and 23.8 widths for compound bends. The mean L_w and *CV* were 11 widths and 0.33, respectively, for simple bends and 13 widths and 0.33, respectively, for compound bends (Fig. 4d).

3.2. Morphological changes

With each sub-bend of compound bends counted independently for analysis of bend morphological change, there were a total of 218 bends in the lower Black River and 157 bends in the lower White River involved (Table 2). It was interesting to note that 16% and 14% of the total number of bends in the lower Black and White rivers, respectively, did not have traceable changes. In both rivers, extension was the most common mode of bend change, which accounted for 46% of bends in the lower Black River and 49% in the lower White River. Translation was also common in both studied reaches, amounting to 18% of the total bends in the lower Black River and 9% in the lower White River. All cases of translation in the two reaches involved bends that migrated towards the downstream direction. ET and TE, as the combination of bend extension and translation, occurred in about 8% and 7%, respectively, of bends in the lower Black River. This compares to about 3% (ET) and 6% (TE) of bends in the lower White River.

In addition to extension, translation, ET, and TE, other types of bend change were rarer in the lower Black River but more common in the lower White River. From 1986 to 2017, the lower Black River only had one case of bend cutoff, whereas the lower White River had nine cases that accounted for 6% of total bends in the studied reach (Table 2). Fifteen cases in the lower White River were classified as "irregular change", which mostly occurred in bends that shared a portion of channel segments with the bends changed by cutoff. Morphological changes of those bends with "irregular change" therefore could not be classified into any of the identified modes. Moreover, retraction, translation with retraction, and bends impacted by lateral changes of bars and islands (marked as "conditional") were relatively rare, in total accounting for 5% and 3% of all bends in the lower Black and White rivers, respectively.

Total migration distances from 1986 to 2017 were statistically summarized among the four major types of meander-bend change: extension, translation, ET, and TE (Fig. 5). In both reaches, the bends changed by translation migrated significantly faster than those changed by extension ($p < 0.05$). The average total migration distances were 0.30 and 0.74 widths for bends that changed by extension in the lower Black and White rivers, respectively, whereas the respective values for bends changed by translation in the two reaches were 0.50 and 1.50 widths. Therefore, the average migration distance of bends changed by translation was about 67% and 103% higher than that of bends changed by extension in the lower Black and White rivers, respectively. Migration distances of bends changed by ET and TE, in general, fell between those of pure extension and translation in both studied reaches, although in the lower White River the mean migration distance of bends changed by ET was as much as that of bends changed by translation (Fig. 5). Overall, meander bends in the lower White River tended to migrate much faster than bends in the lower Black River. On average, the total migration distance of bends in the lower White River was 147%, 206%, 250%, and 159% greater than those of the bends in the lower Black River for bends that changed by extension, translation, ET, and TE, respectively.

For bends that changed by extension and translation, multiple lateral migration rates were associated with a given value of r_m/w (Fig. 6).

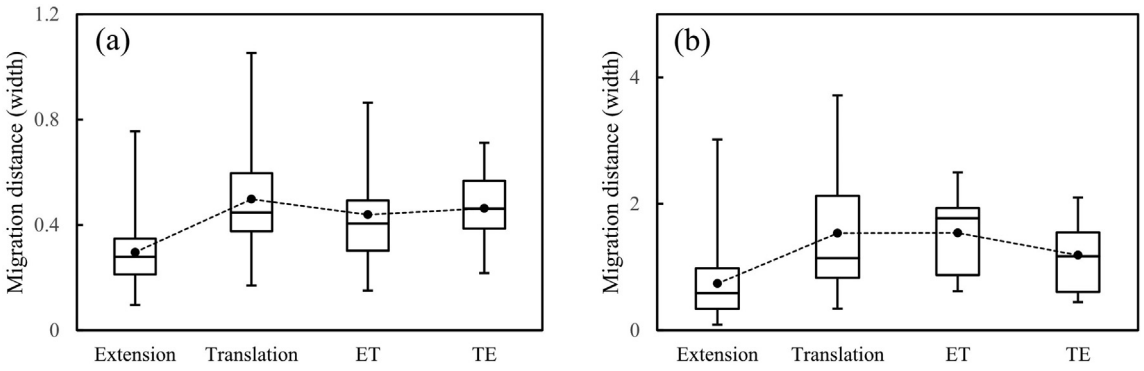

Fig. 5. Data distribution and mean value (dark dots) of width-normalized total migration distance among the four major types of meander-bend change in the studied reaches of the Black River (a) and the White River (b).

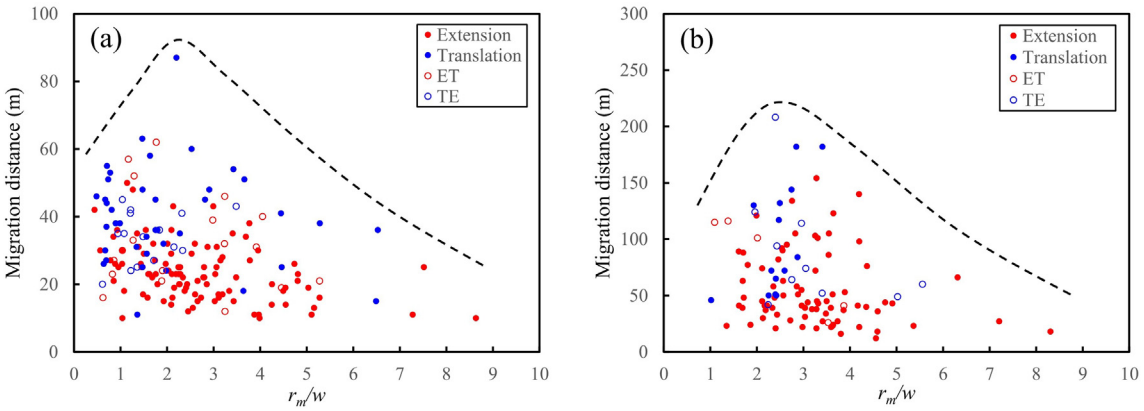

Fig. 6. Relationships between migration distances from 1986 to 2017 of meander bends that changed by the four major modes of bend changes in the studied reaches of the Black River (a) and the White River (b) and r_m/w with the envelope curves.

However, the range of variation increased first with increasing r_m/w, until it reached a value between two and three, and then decreased for the rest of r_m/w values. This pattern may be characterized by a single-mode parabolic envelop (black dotted lines) showing that bend migration reached the maximum when r_m/w = 2-3 in both reaches. In addition, bends that changed by ET and TE were blended into those of the previous two types and followed similar patterns (Fig. 6).

3.3. Morphodynamic patterns

From 1986 to 2017, the total A_e and A_d in the lower Black River were 2.6 and 3 km^2, respectively. For all individual bends along the lower Black River, values of A_e varied within a limited range between zero and 0.04 km^2 with the mean value of 0.012 km^2 and *CV* of 0.58 (Fig. 7a). By contrast, with the mean of 0.014 km^2 and *CV* of 0.89, the longitudinal distribution of A_d in the lower Black River oscillated more widely with higher values prevailing in the downstream portion of the reach. The higher degree of variation for A_d was mostly caused by a few spikes representing substantial deposition in these bends. Some of the bends with larger A_d (i.e., >0.06 km^2) were changed by conditional retraction triggered by the closure of secondary branches previously separated from the main channels by central bars. In general, locations of high and low A_e values were in phase with those of A_d, indicating that lateral migration was primarily achieved by bend lateral movement that involved erosion and deposition to occur separately on the banks (Fig. 7a).

In the lower White River, although the general oscillating patterns of A_e and A_d were similar to those found in the Black River, the degree of oscillation tended to increase longitudinally along the reach (Fig. 7b). Values of both A_e and A_d were constrained in a relatively small range with the mean A_e and A_d of 0.021 and 0.019 km^2, respectively, in the first 50 km. Many spikes were present in the rest downstream portion of the reach, leading to the increased mean values of A_e and A_d (i.e., 0.032 and 0.055 km^2, respectively). Over the entire reach, the total value of A_e and A_d were 3.3 and 4.1 km^2, respectively. The mean A_e and A_d were 0.024 and 0.031 km^2, with their *CV*s of 0.65 and 0.82, respectively. This signified that deposition was the dominant pattern in the studied reach of the White River and that lateral movement was generally greater in the lower White River than that in the lower Black River, a finding consistent with patterns of bend migration.

Longitudinal patterns of A_e/A_d in the two reaches suggested a non-linear decreasing trend in both reaches (Fig. 8). Although the relationship was featured by a discernable degree of scatter and different decreasing ranges, both reaches showed an erosion-dominated pattern in the upstream portion and a deposition-dominated pattern downstream. In the Black River, the turning point for the dominant morphodynamic pattern (i.e., from erosion to deposition-dominated) was about 60 km, the midpoint of the studied reach, indicating a spatially balanced morphodynamic pattern within the reach (Fig. 8a). By contrast, with the turning point for morphodynamic pattern located much more upstream, the lower White River exhibited a strong deposition-dominated trend (Fig. 8b).

4. Discussion

4.1. Relationship between bend curvature and channel migration

The results on the lower Black and White rivers showed that bend migration rates were nonlinearly related to bend curvature (r_m/w) with a migration maxima that occurred around r_m/w = 2.2 and 2.6, respectively, for the two rivers (Fig. 6). Accordingly, bends with both smaller and larger curvatures than the critical value tended to migrate

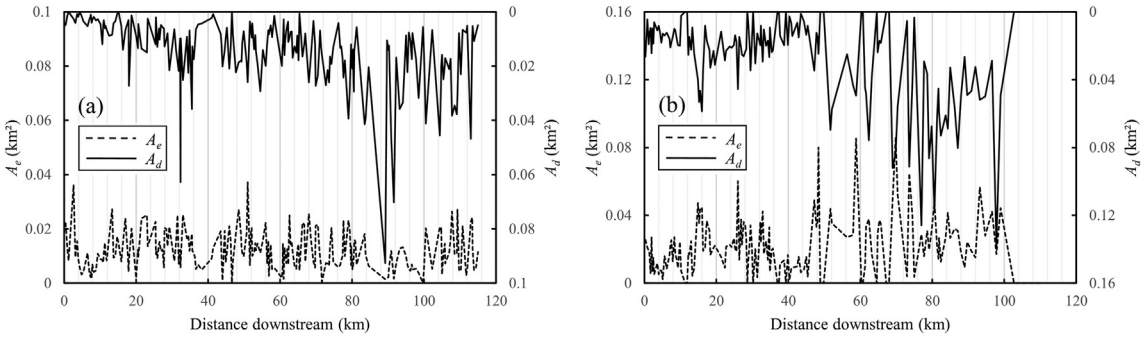

Fig. 7. Longitudinal patterns of A_e and A_d in the studied reaches of the Black River (a) and the White River (b).

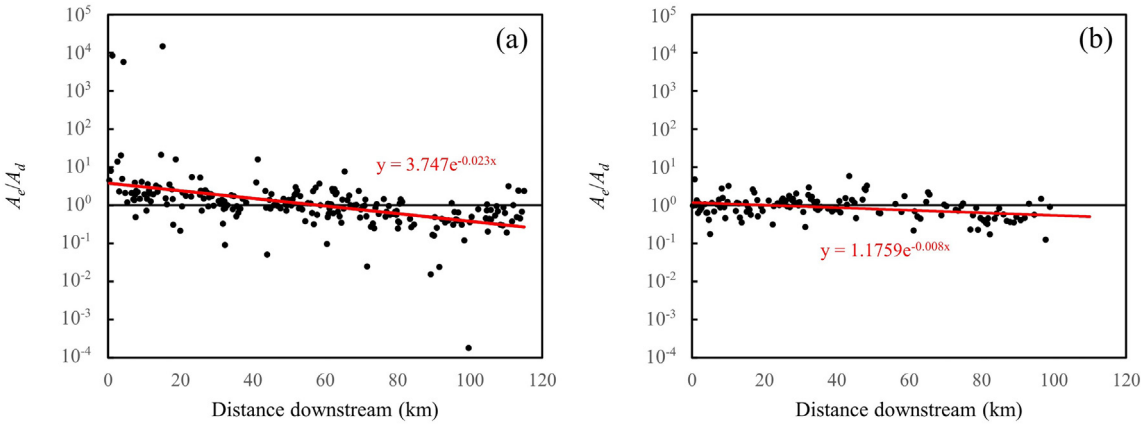

Fig. 8. Longitudinal patterns of ratio A_e/A_d in the studied reaches of the Black River (a) and the White River (b).

more slowly. This pattern was in accord with findings reported in many other meandering rivers (e.g., Hickin and Nanson, 1975; Nanson and Hickin, 1983; Hooke, 1997), which further confirmed the long-standing assertion that bend migration tended to reach the peak in bends with medium curvatures of approximately $r_m/w = 3$ (Hickin, 1978). It should be noted that the relationship between bend curvature and migration rate was obtained from meander bends regardless of their migration modes (e.g., extension and translation). Although earlier modeling studies had supported this conceptual generalization (e.g., Howard and Knutson, 1984), evidence from field studies indicated that this nonlinear pattern between bend curvature and migration rates in fact existed as an envelope covering a wide range of migration rates for a given r_m/w (Hudson and Kesel, 2000; Nicoll and Hickin, 2010; Hooke, 2013; Finotello et al., 2019), as shown in Fig. 6. This pattern between bend curvature and migration rates suggested that meander bends with medium bend curvature were likely to be most capable of eroding banks and reworking floodplains because tightened bends with very high curvature (small r_m/w values) could cause increased flow resistance and partially offset the degree of erosion on the outer banks (Bagnold, 1960; Hickin and Nanson, 1984; Blanckaert and Graf, 2001).

When accounting for the percentage of bends in each r_m/w class interval (every 0.5 of r_m/w value, starting from 0 for the Black River and from 1 for the White River) regarding the total number of bends and calculating the weighted average in each r_m/w interval, we reproduced a curve similar to the classic envelope for both studied reaches (Fig. 9). However, by taking a simple average of migration rates for each class interval of r_m/w, we found that bend migration was, in general, monotonically and inversely related to the curvature with larger migration distance associated with larger curvature (small r_m/w values). This quasi-monotonic and inverse relationship indicated that bends with higher curvature tended to migrate at higher rates, which was supported by a recent study on the meandering tributaries in the Amazon River (Sylvester et al., 2019).

We believe that this apparent discrepancy revealed a fundamental mechanism of bend migration. As a bend tightens with increasing curvature (decreasing r_m/w values), migration of the bend apex is less affected by that of its upstream positions because the bend has short spatial memory (Güneralp and Rhoads, 2009). Thus, a bend with higher curvature (smaller r_m/w) may migrate faster. On the other hand, as bend curvature increases, there may be a higher probability of initiating cutoff to eliminate the entire bend along the meandering channel or triggering compound-form development to stabilize the original bend. This suggests that for a given meandering reach, the number of bends with greater curvature (smaller r_m/w) tends to be fewer than that of bends with smaller curvature (greater r_m/w). This may be perceived as an inherent mechanism of river meandering by which the planform of meander bends stabilizes. Moreover, the peak in the envelope curve that emerged for r_m/w in the range between two and three suggested that the balance between increased flow resistance and fluvial erosion could reach a level leading to the maximum migration rate, although most bends with r_m/w between two and three could not reach this

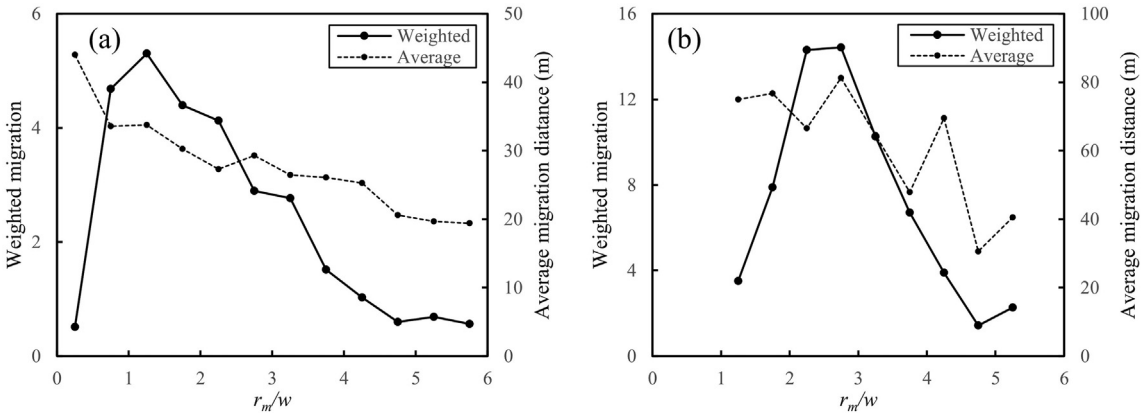

Fig. 9. Average and weighted average migration distances of meander bends that changed by extension, translation, ET, and TE from 1986 to 2017 in the studied reaches of the Black River (a) and the White River (b). Both measures were calculated for every 0.5 increment of r_m/w, starting from 0 for the Black River and from 1 for the White River. Bend curvatures >6 in the Black River and >5.5 in the White River were summarized in the 5.5-6 and 5-5.5 intervals, respectively. Weighted average migration was calculated based on the proportion of the bend number in each class interval to the total number.

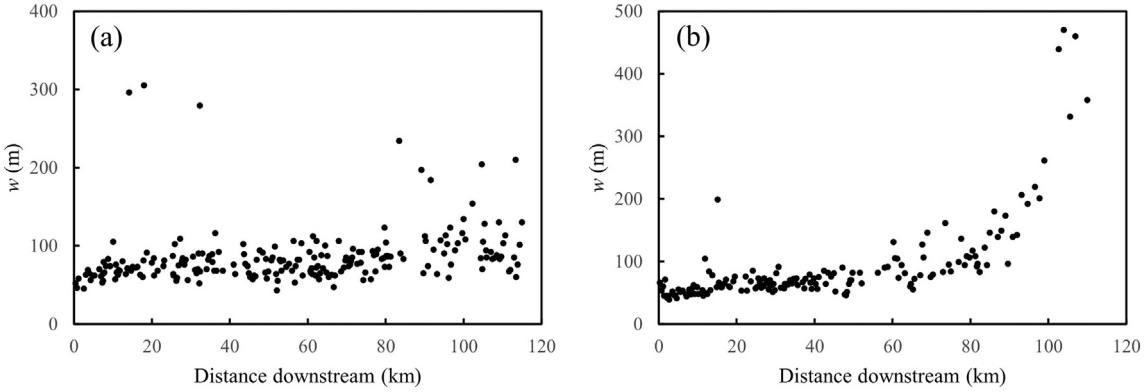

Fig. 10. Longitudinal patterns of channel widths (w) in the studied reaches of the Black River (a) and the White River (b).

level (Fig. 6). Therefore, bend migration is controlled by bend curvature in a complex way that has not yet been fully understood.

4.2. Comparison of bend migration rates between the two studied reaches and with other meandering rivers

Meander bends in the lower Black and White rivers exhibited several distinct morphological characteristics. First, the lower Black River had significantly more compound bends as expressed by both the absolute number (i.e., 50) and the percentage of all bends (i.e., 34%) compared to the lower White River (i.e., 13 and 9%) (Table 1). Additionally, the compound bends in the lower Black River tended to be more complex with more sub-bends and were distributed in clusters. Second, though both A_w and L_w of the compound bends remained generally unchanged along the two studied reaches with higher variations in the Black than in the White River (Fig. 4), the two studied reaches showed significantly different longitudinal trends of w. Although w of the lower Black River only showed a gradual, constant increase throughout the whole reach from about 50 m at the upstream end to about 100 m at the outlet of the river (i.e., 120 km), w of the lower White River increased gradually in the first 40 km but then rose drastically in the lower half of the reach (i.e., after 60 km) (Fig. 10), showing a strong tendency of widening before the river flowed into the Upper Yellow River. Third, the lower White River migrated at a much faster rate than that of the lower Black River. Within the studied period, the mean width-normalized migration distance of bends that changed by extension and translation in the lower White River were 2.5 and 3.1 times, respectively, the migration distance of the lower Black River (Fig. 5). Lastly, only one cutoff occurred in the lower Black River, whereas nine such cases occurred in the lower White River.

Because the two reaches are located in the same area with identical climatic settings and similar hydrogeomorphic properties in terms of the channel size, mean discharge, grain size, and land cover, the most significant difference between the two studied reaches is channel gradient, as the White River is steeper than the Black River. Additionally, though the annual mean discharges of the two rivers were close, the mean annual maximum discharges were 198 and 304 m^3/s for the lower Black and White rivers, respectively. It follows that the maximum unit stream power in the lower White River (13.1 W/m^2) was significantly higher than that of the lower Black River (2.0 W/m^2). Therefore, stream power is likely the critical external factor resulting in the high migration rate and more frequent meander cutoff in the lower White River, as corroborated in many other meandering rivers (Gautier et al., 2007; Nicoll and Hickin, 2010; Hooke, 2013).

On average, meander bends that changed by extension, translation, ET, and TE had migration rates of 0.011 and 0.028 widths/year for the lower Black and White rivers, respectively. To compare with other meandering rivers worldwide in different hydrogeomorphologic settings, we summarized the mean and maximum width-normalized migration rates reported from previous studies (Table 3). Those rivers vary greatly in size and in their environmental settings, such that they represent a sufficiently wide range of natural meandering rivers in the world. We found that lateral migration of the lower Black and White rivers were in the group of rivers with low rates. In particular, the lower Black River had one of the lowest migration rates, suggestive of the slow evolution of the channels and floodplains in this area. However, this comparison is complicated by the inconsistency of the measured migration rates in the selected rivers, which was affected by issues such as: (1) whether width-normalized migration was used; (2) whether lateral migration was measured for entire meandering reaches or only for meander bends; (3) whether the maximum or the average migration distance within the entire course of each bend was used to represent migration distance of the bend for studies focusing on bend-based migration. Migration rates produced in our study are

Table 3
Comparison of width-normalized channel migration rate with other meandering rivers.

	Mean migration (widths/year)	Max migration (widths/year)	Average w (m)	How migration was measured	Reference
Black River	0.011	0.034	86	Maximum	This paper
White River	0.028	0.12	91	Maximum	This paper
Beni River	0.055	0.25	600	Unclear	Gautier et al. (2007)
Lower Mississippi	0.028	0.077	1600	Maximum	Hudson and Kesel (2000)
Tarim River	0.1	2.3	260	Maximum	Li et al. (2017)
Dane River	0.04	0.07	15–20	Unclear	Hooke (2007)
Sacramento River	0.01	0.05	374	Unclear	Micheli et al. (2004)
Canadian Rivers	0.019	0.068	21–288	Maximum	Nicoll and Hickin (2010)
Luangwa River	<0.1	0.22	100–200	Maximum	Gilvear et al. (2000)
Mamoré River	0.05	>0.05	300–500	Average	Constantine et al. (2014)
Solimões–Amazon River	0.005	0.03	>2000	Maximum	Mertes et al. (1996)
Ebro River	0.043	>0.2	200	Maximum	Ollero (2010)

high estimates because we did not include meander bends exhibiting no lateral migration, and we calculated the mean migration rate using the maximum distance of each bends. Nonetheless, lateral migration rates in the Black and White rivers were still generally low compared to the sample of rivers from other regions (Table 3).

5. Conclusions

This study revealed morphological characteristics and patterns of meander-bend changes for two highly convoluted meandering reaches developed in the Zoige Basin within the Qinghai-Tibet Plateau, the highest plateau in the world. These meandering channels were largely undisturbed, providing an opportunity for examining meander morphology and changes controlled by natural fluvial processes. We found that both the Black River and the White River exhibited a tendency of complex planform structures that favored the development of compound bends. This tendency was especially obvious in the Black River with its compound bends accounting for more than one third of total bends. Furthermore, the studied reach of the Black River exhibited relatively slow bend migration and fewer cutoffs than that of the White River, which may be explained by its considerably smaller stream power.

Analysis of bend morphological changes and morphodynamic patterns in the two studied reaches demonstrated that extension, translation, and their combination were the dominant modes of bend change. However, bends that changed by translation tended to migrate at faster rates than those changed by extension. Both reaches had greater areas of deposition than erosion, although both exhibited a transition from an erosion-dominated pattern in the upstream portion into a deposition-dominated pattern in the downstream portion. The relation between bend curvature and migration rates revealed a similar pattern to that of many meandering rivers in other regions, highlighting an envelope curve that shows a peaked migration rate for bends with medium curvatures, commonly between two and three. However, the average migration rates calculated for each class interval of bend curvature showed a quasi-monotonic relationship with bend curvature. Thus, the frequency of bends with similar curvature but different migration rates may alter this envelope relationship, suggesting the complex responses of bend migration to bend planform morphology. The comparison of migration rates with other meandering rivers worldwide showed that the Black and the White rivers were at the higher end of a spectrum of meandering rivers in the world with regards to the complexity of river planform structure. Our results provided new insights into developing complete theories for explaining and predicting bend migration and meander evolution.

Declaration of competing interest

The authors declare that they have no known competing financial interests or personal relationships that could have appeared to influence the work reported in this paper.

Acknowledgements

This study is funded by the Roscoe Martin Fund and the Moynihan/Goekjian Research Grant by the Maxwell School of Citizenship and Public Affairs of Syracuse University, the National Natural Science Foundation of China (51979012), and the Natural Science Foundation of Hubei Province of China (2020CFB554). We thank the editor-in-chief, Scott Lecce, and two reviewers for their constructive comments and suggestions.

References

Alber, A., Piégay, H., 2017. Characterizing and modelling river channel migration rates at a regional scale: case study of south-east France. J. Environ. Manag. 202, 479–493.

Anthony, D.J., Harvey, M.D., 1991. Stage-dependent cross-section adjustments in a meandering reach of Fall River, Colorado. Geomorphology 4 (3-4), 187–203.

Bagnold, R., 1960. Some aspects of the shape of river meanders, U.S. Geol. Surv. Prof. Pap. 282E, 135–144.

Bertoldi, W., Drake, N.A., Gurnell, A.M., 2011. Interactions between river flows and colonizing vegetation on a braided river: exploring spatial and temporal dynamics in riparian vegetation cover using satellite data. Earth Surf. Process. Landf. 36 (11), 1474–1486.

Blanckaert, K., Graf, W.H., 2001. Mean flow and turbulence in open-channel bend. J. Hydraul. Eng. 127 (10), 835–847.

Brice, J.C., 1974. Evolution of meander loops. Geol. Soc. Am. Bull. 85 (4), 581–586.

Casado, A., Peiry, J.L., Campo, A.M., 2016. Geomorphic and vegetation changes in a meandering dryland river regulated by a large dam, Sauce Grande River, Argentina. Geomorphology 268, 21–34.

Chang, H.H., 1984. Analysis of river meanders. J. Hydraul. Eng. 110 (1), 37–50.

Chen, F.H., Bloemendal, J., Zhang, P.Z., Liu, G.X., 1999. An 800 ky proxy record of climate from lake sediments of the Zoige Basin, eastern Tibetan Plateau. Palaeogeogr. Palaeoclimatol. Palaeoecol. 151 (4), 307–320.

Church, M., Ferguson, R.I., 2015. Morphodynamics: rivers beyond steady state. Water Resour. Res. 51 (4), 1883–1897.

Constantine, J.A., Dunne, T., 2008. Meander cutoff and the controls on the production of oxbow lakes. Geology 36 (1), 23–26.

Constantine, J.A., Dunne, T., Ahmed, J., Legleiter, C., Lazarus, E.D., 2014. Sediment supply as a driver of river meandering and floodplain evolution in the Amazon Basin. Nat. Geosci. 7 (12), 899.

Darby, S.E., Alabyan, A.M., Van de Wiel, M.J., 2002. Numerical simulation of bank erosion and channel migration in meandering rivers. Water Resour. Res. 38 (9) (2-1).

Dietrich, W.E., 1987. Mechanics of flow and sediment transport in river bends. River Channels: Environment and Process. vol. 18. Blackwell, Oxford, pp. 179–227.

Dietrich, W.E., Smith, J.D., Dunne, T., 1979. Flow and sediment transport in a sand bedded meander. J. Geol. 87 (3), 305–315.

Donovan, M., Belmont, P., Notebaert, B., Coombs, T., Larson, P., Souffront, M., 2019. Accounting for uncertainty in remotely-sensed measurements of river planform change. Earth Sci. Rev. 193, 220–236.

Downward, S.R., Gurnell, A.M., Brookes, A., 1994. A methodology for quantifying river channel planform change using GIS. IAHS Publications-Series of Proceedings and Reports-Intern Assoc Hydrological Sciences. vol. 224, pp. 449–456.

Ebisemiju, F.S., 1994. The sinuosity of alluvial river channels in the seasonally wet tropical environment: case study of river Elemi, southwestern Nigeria. Catena 21 (1), 13–25.

Ferguson, R.I., 1975. Meander irregularity and wavelength estimation. J. Hydrol. 26 (3–4), 315–333.

Finotello, A., D'Alpaos, A., Lazarus, E.D., Lanzoni, S., 2019. High curvatures drive river meandering: COMMENT. Geology 47 (10), 485.

Frias, C.E., Abad, J.D., Mendoza, A., Paredes, J., Ortals, C., Montoro, H., 2015. Planform evolution of two anabranching structures in the Upper Peruvian Amazon River. Water Resour. Res. 51 (4), 2742–2759.

Frothingham, K.M., Rhoads, B.L., 2003. Three-dimensional flow structure and channel change in an asymmetrical compound meander loop, Embarras River, Illinois. Earth Surf. Process. Landf. 28 (6), 625–644.

Gautier, E., Brunstein, D., Vauchel, P., Roulet, M., Fuertes, O., Guyot, J.L., Darozzes, J., Bourrel, L., 2007. Temporal relations between meander deformation, water discharge and sediment fluxes in the floodplain of the Rio Beni (Bolivian Amazonia). Earth Surf. Process. Landf. 32 (2), 230–248.

Gilvear, D., Bryant, R., 2016. Analysis of remotely sensed data for fluvial geomorphology and river science. In: Kondolf, G.M., Piégay, H. (Eds.), Tools in Fluvial Geomorphology. John Wiley & Sons, Chichester, UK, pp. 103–132.

Gilvear, D., Winterbottom, S., Sichingabula, H., 2000. Character of channel planform change and meander development: Luangwa river, Zambia. Earth Surf. Process. Landf. 25 (4), 421–436.

Güneralp, İ., Marston, R.A., 2012. Process-form linkages in meander morphodynamics: bridging theoretical modeling and real world complexity. Prog. Phys. Geogr. 36 (6), 718–746.

Güneralp, İ., Rhoads, B.L., 2009. Empirical analysis of the planform curvature-migration relation of meandering rivers. Water Resour. Res. 45 (9).

Güneralp, İ., Abad, J.D., Zolezzi, G., Hooke, J., 2012. Advances and challenges in meandering channels research. Geomorphology 163-164, 1–9.

Guo, X., Chen, D., Parker, G., 2019. Flow directionality of pristine meandering rivers is embedded in the skewing of high-amplitude bends and neck cutoffs. Proc. Natl. Acad. Sci. 116 (47), 23448–23454.

Henshaw, A.J., Gurnell, A.M., Bertoldi, W., Drake, N.A., 2013. An assessment of the degree to which Landsat TM data can support the assessment of fluvial dynamics, as revealed by changes in vegetation extent and channel position, along a large river. Geomorphology 202, 74–85.

Hickin, E.J., 1978. Mean flow structure in meanders of the Squamish River, British Columbia. Can. J. Earth Sci. 15 (11), 1833–1849.

Hickin, E.J., Nanson, G.C., 1975. The character of channel migration on the Beaton River, Northeast British Columbia, Canada. Geol. Soc. Am. Bull. 86, 487–494.

Hickin, E.J., Nanson, G.C., 1984. Lateral migration rates of river bends. J. Hydraul. Eng. 110 (11), 1557–1567.

Hooke, J.M., 1984. Changes in river meanders: a review of techniques and results of analyses. Prog. Phys. Geogr. 8 (4), 473–508.

Hooke, J.M., 1997. Styles of channel change. In: Thorne, C.R., Hey, R.D., Newson, M.D. (Eds.), Applied Fluvial Geomorphology for River Engineering and Management. John Wiley & Sons, Chichester, pp. 237–268.

Hooke, J.M., 2007. Complexity, self-organization and variation in behaviour in meandering rivers. Geomorphology 91, 236–258.

Hooke, J.M., 2013. River meandering. In: Shroder, J.F.E.-i.-c., Wohl, E.V.E. (Eds.), Treatise on Geomorphology. Fluvial Geomorphology vol. 9. Academic Press, San Diego, pp. 260–288.
Hooke, J.M., Harvey, A.M., 1983. Meander changes in relation to bend morphology and secondary flows. Modern and Ancient Fluvial Systems, pp. 121–132.
Hooke, J.M., Yorke, L., 2010. Rates, distributions and mechanisms of change in meander morphology over decadal timescales, River Dane, UK. Earth Surf. Process. Landf. 35 (13), 1601–1614.
Howard, A.D., 1992. Modeling channel migration and floodplain sedimentation in meandering streams. In: Carling, P.A., Petts, G.E. (Eds.), Lowland Floodplain Rivers: Geomorphological Perspectives. John Wiley & Sons Ltd., Chichester, UK, pp. 1–41.
Howard, A.D., Knutson, T.R., 1984. Sufficient conditions for river meandering: a simulation approach. Water Resour. Res. 20 (11), 1659–1667.
Hudson, P.F., Kesel, R.H., 2000. Channel migration and meander-bend curvature in the lower Mississippi River prior to major human modification. Geology 28 (6), 531–534.
Ielpi, A., Lapôtre, M.G., 2019. Barren meandering streams in the modern Toiyabe Basin of Nevada, USA, and their relevance to the study of the pre-vegetation rock record. J. Sediment. Res. 89 (5), 399–415.
Ikeda, S., Parker, G., Sawai, K., 1981. Bend theory of river meanders. Part 1. Linear development. J. Fluid Mech. 112, 363–377.
Konsoer, K.M., Rhoads, B.L., Langendoen, E.J., Best, J.L., Ursic, M.E., Abad, J.D., Garcia, M.H., 2016. Spatial variability in bank resistance to erosion on a large meandering, mixed bedrock-alluvial river. Geomorphology 252, 80–97.
Lancaster, S.T., Bras, R.L., 2002. A simple model of river meandering and its comparison to natural channels. Hydrol. Process. 16 (1), 1–26.
Leopold, L.B., Wolman, M.G., 1960. River meanders. Geol. Soc. Am. Bull. 71, 769–793.
Li, Z., Gao, P., 2019a. Channel adjustment after artificial neck cutoffs in a meandering river of the Zoige basin within the Qinghai-Tibet Plateau, China. Catena 172, 255–265.
Li, Z., Gao, P., 2019b. Impact of natural gullies on groundwater hydrology in the Zoige peatland, China. J. Hydrol. Reg. Stud. 21, 25–39.
Li, Z., Yu, G.A., Brierley, G.J., Wang, Z., Jia, Y., 2017. Migration and cutoff of meanders in the hyperarid environment of the middle Tarim River, northwestern China. Geomorphology 276, 116–124.
Li, Z., Gao, P., You, Y., 2018. Characterizing hydrological connectivity of artificial ditches in Zoige Peatlands of Qinghai-Tibet Plateau. Water 10 (10), 1364.
Li, Z., Gao, P., Hu, X., Yi, Y., Pan, B., You, Y., 2019. Coupled impact of decadal precipitation and evapotranspiration on peatland degradation in the Zoige basin, China. Phys. Geogr. 41 (2), 145–168.
Magdaleno, F., Fernández-Yuste, J.A., 2011. Meander dynamics in a changing river corridor. Geomorphology 130 (3-4), 197–207.
Markham, A.J., Thorne, C.R., 1992. Geomorphology of gravel-bed river bends. Dynamics of Gravel-bed rivers, pp. 433–450.
Mertes, L.A., Dunne, T., Martinelli, L.A., 1996. Channel-floodplain geomorphology along the Solimões-Amazon river, Brazil. Geol. Soc. Am. Bull. 108 (9), 1089–1107.
Micheli, E.R., Kirchner, J.W., Larsen, E.W., 2004. Quantifying the effect of riparian forest versus agricultural vegetation on river meander migration rates, Central Sacramento River, California, USA. River Res. Appl. 20 (5), 537–548.
Morais, E.S., Rocha, P.C., Hooke, J., 2016. Spatiotemporal variations in channel changes caused by cumulative factors in a meandering river: the lower Peixe River, Brazil. Geomorphology 273, 348–360.
Nanson, G.C., 1980. Point bar and floodplain formation of the meandering Beatton River, northeastern British Columbia, Canada. Sedimentology 27 (1), 3–29.
Nanson, G.C., Hickin, E.J., 1983. Channel migration and incision on the Beatton river. J. Hydraul. Eng. 109 (3), 327–337.
Nicoll, T.J., Hickin, E.J., 2010. Planform geometry and channel migration of confined meandering rivers on the Canadian prairies. Geomorphology 116 (1-2), 37–47.
Nicoll, T., Brierley, G.J., Yu, G.A., 2013. A broad overview of landscape diversity of the Yellow River source zone. J. Geogr. Sci. 23, 793–816.
Ollero, A., 2010. Channel changes and floodplain management in the meandering middle Ebro River, Spain. Geomorphology 117 (3-4), 247–260.
Parker, G., Diplas, P., Akiyama, J., 1983. Meander bends of high amplitude. J. Hydraul. Eng. 109 (10), 1323–1337.
Perucca, E., Camporeale, C., Ridolfi, L., 2007. Significance of the riparian vegetation dynamics on meandering river morphodynamics. Water Resour. Res. 43 (3).
Qiu, P., Wu, N., Luo, P., Wang, Z., Li, M., 2009. Analysis of dynamics and driving factors of wetland landscape in Zoige, Eastern Qinghai-Tibetan Plateau. J. Mt. Sci. 6 (1), 42–55.
Schumm, S.A., 1985. Patterns of alluvial rivers. Annu. Rev. Earth Planet. Sci. 13 (1), 5–27.
Schwendel, A.C., Nicholas, A.P., Aalto, R.E., Sambrook Smith, G.H., Buckley, S., 2015. Interaction between meander dynamics and floodplain heterogeneity in a large tropical sand-bed river: the Rio Beni, Bolivian Amazon. Earth Surf. Process. Landf. 40 (15), 2026–2040.
Schwenk, J., Khandelwal, A., Fratkin, M., Kumar, V., Foufoula-Georgiou, E., 2017. High spatiotemporal resolution of river planform dynamics from landsatLandsat: the RivMAP toolbox and results from the Ucayali river. Earth Space Sci. (Hoboken, N.J.) 4 (2), 46–75.
Seminara, G., 2006. Meanders. J. Fluid Mech. 554, 271–297.
Simon, A., Collison, A.J., 2002. Quantifying the mechanical and hydrologic effects of riparian vegetation on streambank stability. Earth Surf. Process. Landf. 27 (5), 527–546.
Stølum, H.H., 1996. River meandering as a self-organization process. Science 271 (5256), 1710–1713.
Sylvester, Z., Durkin, P., Covault, J.A., 2019. High curvatures drive river meandering. Geology 47 (3), 263–266.
Thorne, C.R., 1991. Bank erosion and meander migration of the Red and Mississippi Rivers, USA. Hydrology for the Water Management of Large River Basins: 20th General Assembly of the International Union of Geodesy and Geophysics, Vienna. International Association of Hydrological Sciences, pp. 301–313.
Winterbottom, S.J., 2000. Medium and short-term channel planform changes on the Rivers Tay and Tummel, Scotland. Geomorphology 34 (3-4), 195–208.
Yousefi, S., Pourghasemi, H.R., Hooke, J., Navratil, O., Kidová, A., 2016. Changes in morphometric meander parameters identified on the Karoon River, Iran, using remote sensing data. Geomorphology 271, 55–64.
Zinger, J.A., Rhoads, B.L., Best, J.L., Johnson, K.K., 2013. Flow structure and channel morphodynamics of meander bend chute cutoffs: a case study of the Wabash River, USA. J. Geophys. Res. Earth Surf. 118 (4), 2468–2487.
Zolezzi, G., Seminara, G., 2001. Downstream and upstream influence in river meandering. Part 1. General theory and application to overdeepening. J. Fluid Mech. 438 (13), 183–211.